

# On the Airborne Spatial Coverage Requirement for Microwave Satellite Validation

Christoph Rüdiger, *Member, IEEE*, Jeffrey P. Walker, and Yann H. Kerr, *Senior Member, IEEE*

**Abstract**—With the recent launch of the Soil Moisture and Ocean Salinity (SMOS) mission, the passive microwave remote-sensing community is currently planning and undertaking airborne validation campaigns. Given the financial and logistical constraints on the size of validation area that can be covered by airborne simulators and the experiments underway that cover only a part of a satellite footprint, timely and scientifically sound advice on fractional footprint coverage requirements by campaigns for these low-resolution sensors is of paramount importance. Using high-resolution airborne data from an extensive airborne campaign in Southeast Australia, the fractional coverage requirement for L-band passive microwave satellite missions is assessed using a subsampling technique of flight lines through a passive microwave footprint. It is shown that minimum 50% coverage of the total footprint size will typically be required, given a spatial variability value of 20 K at 1-km resolution, to ensure that the footprint mean is estimated with an expected sampling error of less than 4 K, which is the design sensitivity of SMOS.

**Index Terms**—Airborne validation, passive microwave remote sensing, Soil Moisture and Ocean Salinity (SMOS), spatial requirements.

## I. INTRODUCTION

THREE important satellite missions to monitor the hydrologic state of the terrestrial surface are under development or have recently been launched. These are the European Space Agency-led Soil Moisture and Ocean Salinity (SMOS) mission [1] launched on November 2, 2009; the joint National Aeronautics and Space Administration (NASA) and Argentinean National Space Activities Commission Aquarius mission with an expected launch in 2011 [2]; and NASA's Soil Moisture Active Passive (SMAP) mission scheduled for launch in 2014 [3]. All three satellites will be operating within a scarcely utilized L-band (1.4 GHz) microwave range using untested (in space) technology, therefore requiring extensive ground validation campaigns. The only passive L-band space measurements prior to SMOS was the Skylab mission, which collected data for a number of transects over several years of operation from

1973 to 1977 [4], [5]. Consequently, many ground validation campaigns are being planned to ensure that the satellite measurements of microwave brightness temperature and the derived soil moisture products are of high quality (see [6]). However, due to financial and logistical constraints, many of these campaigns are planning to only partly cover the satellite footprint(s) to be validated with aircraft sensors. Apart from the practical limitation that many of the airborne instruments available only measure a single line of data (e.g., EMIRAD [7]), meaning that they cannot be used to fully cover an entire satellite footprint within a reasonable time duration of a satellite overpass, there has typically been a conscious decision to focus on maximizing the area covered within the limitations of the technical constraints of the instruments used or according to the experiment requirements, e.g., to have a high number of repeat flights at the expense of spatial coverage or have spatial coverage at the expense of spatial resolution. Hence, field campaigns are generally being planned to be spatially limited to a single footprint or a part thereof, or a single/few flight transects across a number of footprints, with the explicit assumption that the collected data are representative of the mean response measured by the satellite for those footprints. However, until now, there has been no rigorous assessment of the likely impact that such campaign designs will have on the eventual satellite validation results.

Some of the most widely known field campaigns conducted in recent years are the Soil Moisture Experiments in the USA [8], the REMEDHUS network of the University of Salamanca in Spain [9], and the National Airborne Field Experiments (NAFE) in Southeast Australia [10], [11], which have included the use of airborne microwave radiometers. While these experiments have collected extensive ground-based and airborne data essential to the development of soil moisture remote-sensing and downscaling algorithms, it is important to note that those experiments did not collect the type of data required for the study undertaken here, requiring full coverage of observed microwave emission at high resolution across the entire satellite-sized pixels that include a wide range of surface types and environmental conditions. Consequently, they are not well suited in making an assessment of ground validation campaign design and/or the fractional coverage requirement of satellite footprints to achieve a reliable estimate of the mean microwave emission of a satellite footprint. However, a recent campaign undertaken in Southeast Australia, specifically designed for the validation of SMOS (the Australian Airborne Calibration/Validation Experiment for SMOS (AACES) [12]), provides a unique opportunity to address this important question. This campaign mapped L-band microwave emission from more than 20 independent SMOS-sized footprints across an area of 500 ×

Manuscript received October 17, 2010; revised January 5, 2011 and February 7, 2011; accepted February 11, 2011. Date of publication March 23, 2011; date of current version June 24, 2011. The work of C. Rüdiger was supported by the Australian Research Council Discovery Project under Grant DP0879212.

C. Rüdiger and J. P. Walker are with the Department of Civil Engineering, Monash University, Clayton, VIC 3800, Australia (e-mail: chris.rudiger@monash.edu).

Y. H. Kerr is with the Centre d'Etudes Spatiales de la Biosphère (CESBIO), Centre National de Recherches Scientifiques, Centre National d'Etudes Spatiales, Université Paul Sabatier, Institut de Recherche pour le Développement (CNRS-CNES-UPS-IRD), 31401 Toulouse, France.

Color versions of one or more of the figures in this paper are available online at <http://ieeexplore.ieee.org>.

Digital Object Identifier 10.1109/LGRS.2011.2116766

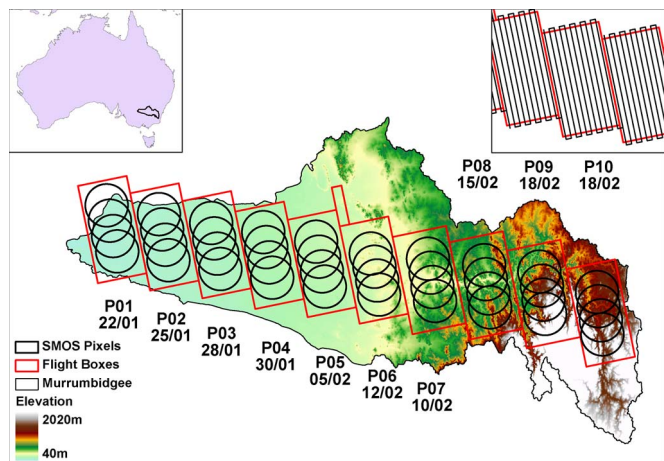


Fig. 1. Elevation map of the Murrumbidgee River catchment and the airborne focus areas, with the top-left insert showing the location of the catchment (black line) within Australia. The circles represent the locations of SMOS pixels entirely located within the focus areas (red boxes). The individual flight transects of each focus area are shown as black lines within the insert to the top right.

100 km, with a wide range of environmental conditions typical of both semi-arid and temperate climates. Consequently, this letter takes advantage of this extensive airborne data set to study the satellite footprint coverage required to achieve a brightness temperature sampling uncertainty of not more than 4 K, which is the uncertainty requirement for passive microwave measurements over land to achieve a soil moisture retrieval error of less than  $0.02 \text{ m}^3/\text{m}^3$  for bare and moderately humid soils (approximately  $0.03 \text{ m}^3/\text{m}^3$  for herbaceous vegetation and  $0.06 \text{ m}^3/\text{m}^3$  for dense forests). As soil moisture retrieval algorithms introduce errors and uncertainties of their own, this letter focuses on brightness temperature data as the only direct physical measurement.

## II. STUDY SITE AND THE DATA SET

### A. Murrumbidgee River Catchment

The data set used in this letter was collected during the AACES [12], which took place from January 18, 2010 to February 21, 2010 and September 8–26, 2010 in the Murrumbidgee River catchment in Southeast Australia. The catchment is located between  $34^\circ$  and  $36^\circ$  southern latitude and between  $143^\circ$  and  $150^\circ$  eastern longitude, encompassing a large variety of low-level plains in the west to alpine conditions in the east (see Fig. 1). The western areas are predominantly used for grazing, whereas cropping is more dominant in the central part (particularly in the Murrumbidgee and Coleambally Irrigation Areas) and transitioning to woody vegetation in the east of the catchment. While the western half of the Murrumbidgee River catchment is flat, the eastern quarter is dominated by undulating-to-rugged alpine conditions. The central irrigation districts were studied during the NAFE 2006 campaign [11].

Due to its distinctive topography, the Murrumbidgee River catchment exhibits significant spatial variability in climate, topography, soil type, vegetation type, and land use. This makes the region an ideal test bed for comprehensive validation of passive microwave missions, due to the diversity within this area, the large amount of complementary data from long-term

monitoring sites, and other airborne field experiments in the catchment. It is also highly complementary to the study sites in other countries.

### B. L-Band Brightness Temperatures

The data set analyzed in this letter consists of vertically and horizontally polarized passive L-band brightness temperatures, which are collected with the Polarimetric L-band Multibeam Radiometer (PLMR) at  $1.413 \text{ GHz} (\pm 12 \text{ MHz})$  [10], which has been used extensively throughout the NAFE campaigns [10], [11]. The data collected with the PLMR during the NAFE campaigns were used in a number of studies on downscaling low-resolution data [13], radiative transfer model validation [14], [15], and comparison studies with high-resolution satellites [16]. The PLMR has a calibration accuracy of  $< 2 \text{ K}$  (based on an analysis of multiple years of calibration data, using hot and cold calibration targets) [10]. The data used in this letter were obtained by flying the PLMR at an altitude of approximately 3000 m above the ground level, resulting in a nominal ground resolution of 1 km for each of six across-track pixels and a sampling rate of  $\sim 40 \text{ m}$  for along-track pixels. Six digitally formed antenna beams of the PLMR result in a total swath width of nominally 6 km for each transect, with a 1-km overlap for adjacent flight lines.

The flights took place over a 4–5-h window, which is centered on the local SMOS ascending overpass time of  $\sim 6 \text{ A.M.}$  Ground-based monitoring stations simultaneously monitored the diurnal changes of soil moisture and temperature within the flight area at various locations and depths. These observations were then used to correct any brightness temperature variation during the flight due to soil temperature and moisture changes over that period. To correct for angular differences, the mean of the data collected with each beam was scaled to the mean of the data collected with the outer PLMR beams ( $38^\circ$ ), similar to [17], as this value is the incidence angle found in the majority of the SMOS scenes and approximates the incidence angle of SMAP. Moreover, part of the first flight line was repeated at the end of the flight to confirm the temporal correction procedure.

Two independent or a total of four complete SMOS footprints were observed during each flight, for an area of  $50 \times 100 \text{ km}$  (see Fig. 1). Note that the SMOS data grid is computed on a regular grid of 15-km spacing, resulting in an overlap of individual SMOS footprints each being  $\sim 42 \text{ km}$  in diameter. To cover the entire catchment, ten such flights were undertaken (five during the winter campaign, covering the central five focus areas P04–P08). As each flight transect was designed to overlap the outer beam measurements of adjacent flight lines, a total of ten flight lines of a length of 100 km each was required to cover the 50-km-wide focus areas. The flight lines were aligned with the SMOS grid, so that the maximum number of entire SMOS pixels fell within the focus areas. The variation of the surface conditions is further highlighted in Table I, comparing the different surface conditions across the ten focus areas.

The first four flights were undertaken under very dry and hot conditions. This was followed by two significant rain events (on February 2 and 13, before the flights scheduled for P05 and P08, respectively), leading to significant wetting and subsequent dry down of various parts of the catchment. These weather conditions provided a fortuitous opportunity to assess spatial

TABLE I  
DOMINANT VEGETATION [18], SOIL CHARACTERISTICS [19], AND  
AVERAGE TERRAIN ALTITUDE ACROSS THE TEN FOCUS AREAS

Focus Area	Soils *	Vegetation **	Terrain Altitude [m] ***
P01	6.2 / 62.7 / 30.6	77.4 / 17.4 / 2.8	60
P02	0 / 100 / 0	96.6 / 1.7 / 1.4	75
P03	0 / 65.5 / 34.5	96.5 / 0.7 / 2.6	90
P04	0 / 16.8 / 83.2	89.1 / 10.3 / 0.2	105
P05	0 / 0 / 98.9	42.7 / 54.4 / 0.2	120
P06	4.9 / 0 / 94.9	34.1 / 61.5 / 3.0	150
P07	2.4 / 0 / 97.0	41.4 / 56.2 / 1.6	240
P08	0 / 0 / 97.1	54.7 / 41.7 / 3.5	330
P09	0 / 0 / 99.7	36.6 / 23.6 / 38.4	585
P10	0 / 0 / 99.8	29.6 / 28.5 / 33.7	600

\* remaining fractions are undefined soil types

\*\* remaining fractions are open water bodies and urban areas

\*\*\* average altitude above sea level across the focus area

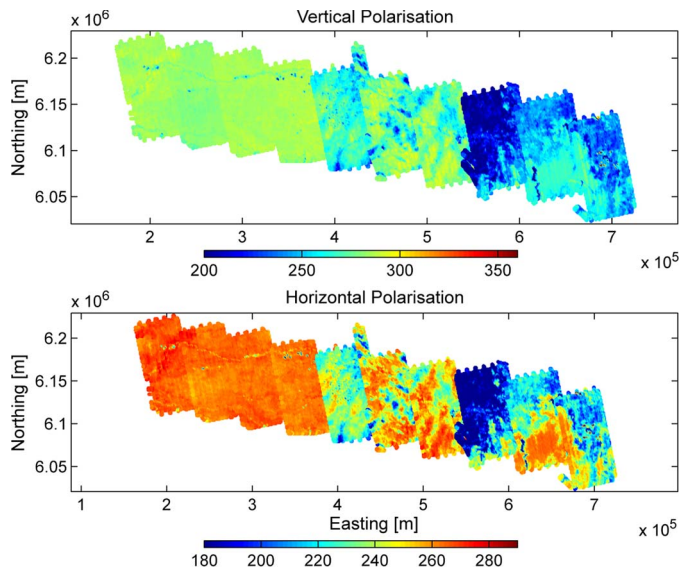


Fig. 2. Spatial variation of the vertical (top) and horizontal (bottom) polarized brightness temperatures  $K$  collected throughout the focus areas in Fig. 1 across the Murrumbidgee River catchment between January 22, 2010 and February 18, 2010.

variability under a wide range of environmental conditions, including hot and dry through humid and cool. In contrast, the Australian winter of 2010 was remarkably wet resulting in high soil moisture content throughout the catchment and also significant vegetation cover and therefore significantly changing the surface conditions between summer and winter campaigns, further broadening the spectrum of different surface conditions to be assessed. Fig. 2 shows the horizontally and vertically polarized brightness temperature data sets (summer only), with low brightness temperatures toward the east in response to rainfall being clearly obvious. These conditions together with flat terrain and low vegetation biomass resulted in very small spatial variability of brightness temperature observed across the first four focus areas (see Table II). However, the patchiness of rainfall, together with a greater variation in topography, soils, and land use and the forested areas in the focus areas toward the far east, resulted in more typical spatial variability in the six eastern flights over the catchment.

TABLE II  
STATISTICS OF THE VERTICALLY AND HORIZONTALLY POLARIZED  
BRIGHTNESS TEMPERATURES OBSERVED WITHIN THE INDIVIDUAL  
FOCUS AREAS (BOTH SUMMER AND WINTER PERIODS),  
CALCULATED FROM 1-KM RESOLUTION DATA

Focus Area	v-pol		h-pol	
	Mean [K]	Std. Dev. [K]	Mean [K]	Std. Dev. [K]
P01	284.0	3.87	266.2	5.07
P02	281.0	2.65	263.0	3.81
P03	284.6	2.60	264.0	3.16
P04 – summer	285.3	4.85	262.2	6.02
P04 – winter	223.7	16.1	195.4	16.0
P05 – summer	257.4	14.3	230.3	14.5
P05 – winter	218.0	20.1	187.4	19.9
P06 – summer	270.9	16.9	244.9	18.8
P06 – winter	231.0	16.0	201.1	16.4
P07 – summer	275.2	12.1	252.2	14.8
P07 – winter	230.4	12.3	202.6	12.7
P08 – summer	219.6	22.0	194.2	24.9
P08 – winter	232.9	10.6	212.5	12.4
P09	252.2	15.8	237.7	22.9
P10	246.9	18.5	226.7	22.8

### III. ANALYSIS

To study the fractional coverage requirement for microwave satellite footprints to accurately estimate the spatial mean, a subsampling technique was used. Consequently, all possible combinations of partial footprint coverage by flight lines through each flight coverage were assessed. The true mean (and standard deviation) of each individual focus area was assumed to be that calculated from the entire coverage of the focus areas (see Table II). This approach was chosen, rather than using the exact shape and size of the SMOS footprints, for the sake of simplicity and because the added complexity would not alter the key conclusions of this letter. Moreover, this approach still ensures that the full variability within a satellite-sized footprint is captured. The mean and standard deviations of all possible transect combinations were then calculated using data from 1 to  $n$  transects of the  $n$  transects covering each individual focus area (e.g., using transects 1 and 2, 1 and 3, ..., 5 and 10, etc., for the combination of only two individual transects for the calculations).

A maximum sampling error of 4 K was selected as the target uncertainty requirement for this letter as this is the passive microwave measurement accuracy required over land to achieve a soil moisture error of approximately  $0.02 \text{ m}^3/\text{m}^3$  for bare soils and to match the design radiometric sensitivity of SMOS [1]. Consequently, plotting the fractional area covered by the transect combinations against the departure from the overall mean allows an assessment to be made of when the required level of sampling accuracy is achieved. This was assumed to be the case, when a confidence interval of 90% of the standard deviation for all flight line combinations of the  $n$ th number of transects within a footprint (and consequently the spatial coverage) was within the 4 K requirement.

Fig. 3 shows the plots of the aforementioned analysis alongside a spatial overview of the data collected within each focus area for the horizontal polarization (the vertical polarization is not shown here as the distributions are almost identical).

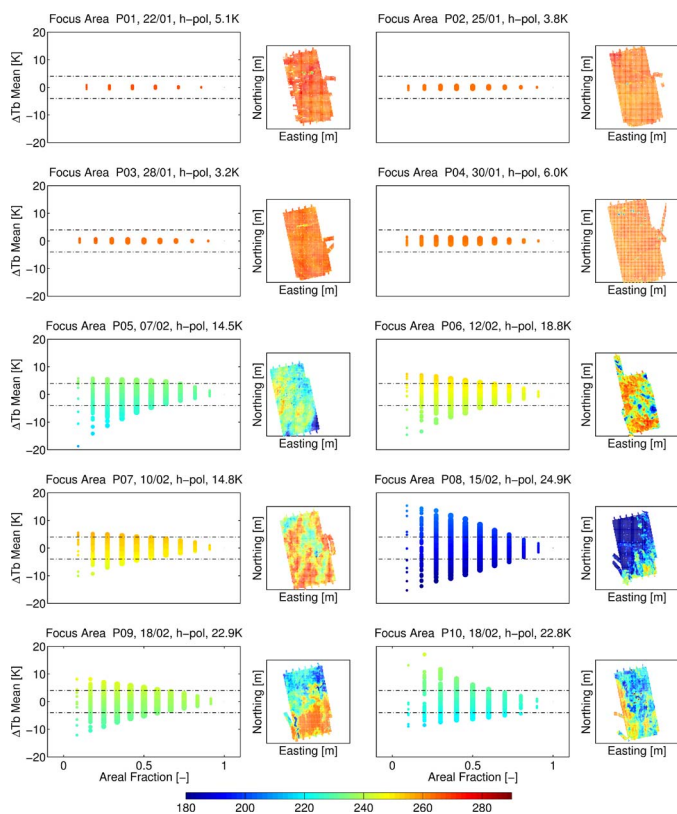


Fig. 3. Sampling error in the horizontally polarized data due to partial coverage (scatter plots) and spatial variation in brightness temperature (brightness temperature maps) for each of the ten focus areas covered during AACES (P01–P10). Color shading is according to the observed brightness temperature, and the size of the markers on the scatter plots is a function of the total number of possible transect combinations with that of error and area, respectively. The horizontal lines represent the target error margin of 4 K from the mean observed brightness temperature. Note that the color scale for P08 was saturated due to the wet soil conditions and was not changed to preserve the details in the remaining nine plots.

The results show that data collected during the first four flight operation days of the campaign could have been represented by a single transect as the average of any of those transect combinations falls within the range of  $\pm 4$  K. This is due to the semi-arid landscape in the area coupled with very hot (in excess of  $40\text{ }^{\circ}\text{C}$ ) and dry conditions (below  $0.10\text{ m}^3/\text{m}^3$  soil moisture content), leading to uniform emission properties.

The remaining focus areas exhibit a very different and more typical behavior for temperate climates in their departure from the mean brightness temperature. These areas exhibit wider variability in land use and land cover similar to those of agricultural areas around the globe. Moreover, at the time of sampling, they were in an intermediate-to-wet condition due to the rainfall events during the middle of the campaign. While it may be postulated that “random” rainfall events will lead to a random surface soil-moisture field and, consequently, the same mean brightness temperature response for each transect, the data collected across focus areas 5–10 show that this not to be the case, with the spread of the mean brightness temperatures being large for any combination of transects covering less than about half of the entire area of each focus area. The patchiness of brightness temperature is in part due to differences in the soil properties (and, consequently, a spatially variable dry down) but also, in

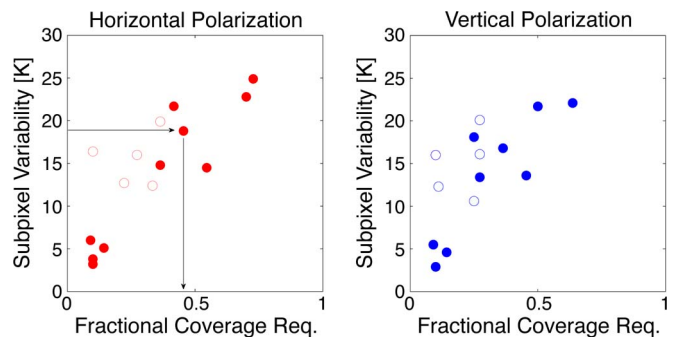


Fig. 4. Scatter plot showing the spatial variability in brightness temperature across the microwave footprint (as calculated from a 1-km grid) against the fraction of total area coverage required to achieve an accuracy of 4 K for both vertical and horizontal polarizations. The arrows show an example of how this chart could be used to estimate the required fractional coverage for a known subpixel variability value. The filled and empty markers represent the summer and winter campaign data, respectively.

a lesser part, due to the spatial distribution of vegetation cover and topographic conditions. However, the dominant effect seen in the brightness temperatures for areas 5–10 are the significant rain events that are more relevant here than any topographic or vegetation effect. The latter is particularly obvious in the higher brightness temperatures of the eastern focus areas, where forests are the dominating vegetation feature in the southern part of the focus areas. While particular consideration may be given to somewhat extreme examples such as those both in the sampling design and the subsequent analysis, there are many other examples with more “normal” conditions that also show sampling of less than half of a microwave footprint, and use of a single transect in particular may lead to large errors. The results in Fig. 3 show that, if a single transect is used, the average brightness temperature may be overestimated or underestimated by as much as 25 K, consequently leading to a potentially significant misinterpretation of the accuracy of the spaceborne observations. Fig. 4 summarizes Fig. 3 with the addition of the winter campaign data, showing the coverage requirement to achieve an accuracy of 4 K according to subpixel variability. For example, the arrows on Fig. 4 show that for focus area 6 (summer campaign), with subpixel variability of about 19 K, the required coverage is 45% in order to achieve a departure of less than 4 K from the mean estimated by full coverage. While these results may seem intuitive, they serve to demonstrate the importance of adequate campaign design and the significant estimation error that can result if arbitrary (based on monitoring station locations) transects are used in isolation to estimate the satellite footprint brightness temperature averages. Moreover, the fact that the winter campaign data (with their significantly different surface conditions) have the same tendency highlights the fact that these correlations are not a coincidence. Consequently, experimental analysis of satellite missions based on such campaign design cannot be relied upon without careful consideration of how to account for the misrepresentation of the observed data.

While it may be argued that validation of the soil moisture product based on the retrieval of the PLMR data via a radiative transfer model and the SMOS soil moisture product may not result in such significant spatial variations, this letter solely deals

with the validation of the satellite measurements of brightness temperature. Validation of the higher level retrieval products can only be performed once the Level-1 brightness temperature data have been adequately validated itself.

#### IV. CONCLUSION

This letter has assessed the requirements for airborne validation campaigns of new microwave remote-sensing satellites. Brightness temperature data from an extensive airborne experiment undertaken in Southeast Australia with an unprecedented spatial extent have been used in this letter. The campaign covered more than 20 independent satellite-sized passive microwave footprints, which were used to quantify the spatial coverage required to achieve an estimate of the satellite footprint mean with an expected sampling error of less than 4 K, which is the design sensitivity of SMOS and also the uncertainty requirement to achieve a soil moisture error of less than  $0.02 \text{ m}^3/\text{m}^3$  for bare soils from passive microwave remote sensing. It was found that, for areas with typical spatial variability, being on the order of 20 K (as derived from a 1-km grid), at least 50% coverage is required to achieve this goal irrespective of the vegetation and topographic conditions within the catchment. Consequently, if there is no prior knowledge of the spatial variability of the satellite footprint being assessed, at least 50% of the footprint should be covered to guarantee that the mean footprint microwave emission can be accurately determined. Moreover, if there are large portions of highly contrasting areas (e.g., forest and grazing) within the footprint, flight line planning should ensure that both areas are covered in proportion to their spatial contributions. However, in the case of very flat homogenous areas following long dry spells, the footprint average can be well characterized from a single transect across the area, providing that there have not been any recent localized storms.

While it may be possible to use these data to develop optimized sampling theorems that would allow the calculation of an average from the reduced coverage, it has to be pointed out that this is not the intention of this letter. It is rather intended to warn that great care is required when undertaking field validation campaigns with less than full coverage.

#### REFERENCES

- [1] Y. H. Kerr, P. Waldteufel, J.-P. Wigneron, S. Delwart, F. Cabot, J. Boutin, M.-J. Escorihuela, J. Font, N. Reul, C. Gruhier, S. E. Juglea, M. R. Drinkwater, A. Hahne, M. Martín-Neira, and S. Mecklenburg, "The SMOS mission: New tool for monitoring key elements of the global water cycle," *Proc. IEEE*, vol. 98, no. 5, pp. 666–687, May 2010.
- [2] D. M. Le Vine, G. S. E. Lagerloef, F. R. Colomb, S. H. Yueh, and F. A. Pellerano, "Aquarius: An instrument to monitor sea surface salinity from space," *IEEE Trans. Geosci. Remote Sens.*, vol. 45, no. 7, pp. 2040–2050, Jul. 2007.
- [3] D. Entekhabi, E. G. Njoku, P. E. O'Neill, K. H. Kellogg, W. T. Crow, W. N. Edelstein, J. K. Entin, S. D. Goodman, T. J. Jackson, J. Johnson, J. Kimball, J. R. Piepmeier, R. D. Koster, N. Martin, K. C. McDonald, M. Moghaddam, S. Moran, R. Reichle, J. C. Shi, M. W. Spencer, S. W. Thurman, L. Tsang, and J. Van Zyl, "The Soil Moisture Active Passive (SMAP) mission," *Proc. IEEE*, vol. 98, no. 5, pp. 704–716, May 2010.
- [4] J. R. Eagleman and W. C. Lin, "Remote sensing of soil moisture by a 21-cm passive radiometer," *J. Geophys. Res.*, vol. 81, no. 21, pp. 3660–3666, 1976.
- [5] M. Drusch, T. Holmes, P. de Rosnay, and G. Balsamo, "Comparing ERA-40-based L-band brightness temperatures with Skylab observations: A calibration/validation study using the community microwave emission model," *J. Hydromet.*, vol. 10, no. 1, pp. 213–226, 2009.
- [6] S. Delwart, C. Bouzinac, P. Wursteisen, M. Berger, M. Drinkwater, M. Martín-Neira, and Y. H. Kerr, "SMOS validation and the COSMOS campaigns," *IEEE Trans. Geosci. Remote Sens.*, vol. 46, no. 3, pp. 695–704, Mar. 2008.
- [7] N. Skuo, B. Laursen, and S. Søjbjerg, "Polarimetric radiometer configurations: Potential accuracy and sensitivity," *IEEE Trans. Geosci. Remote Sens.*, vol. 37, no. 5, pp. 2165–2171, Sep. 1999.
- [8] E. G. Njoku, T. J. Jackson, V. Lakshmi, T. K. Chan, and S. V. Nghiem, "Soil moisture retrieval from AMSR-E," *IEEE Trans. Geosci. Remote Sens.*, vol. 41, no. 2, pp. 215–229, Feb. 2003.
- [9] J. Martínez-Fernández and A. Ceballos, "Mean soil moisture estimation using temporal stability analysis," *J. Hydrol.*, vol. 312, no. 1–4, pp. 28–38, Oct. 2005.
- [10] R. Panciera, J. P. Walker, J. D. Kalma, E. J. Kim, J. M. Hacker, O. Merlin, M. Berger, and N. Skou, "The NAFE'05/CoSMOS data set: Towards SMOS soil moisture retrieval, downscaling, and assimilation," *IEEE Trans. Geosci. Remote Sens.*, vol. 46, no. 3, pp. 736–745, Mar. 2008.
- [11] O. Merlin, J. P. Walker, J. D. Kalma, E. J. Kim, J. Hacker, R. Panciera, R. Young, G. Summerell, J. Hornbuckle, M. Hafeez, and T. Jackson, "The NAFE'06 data set: Towards soil moisture retrieval at intermediate resolution," *Adv. Water Resour.*, vol. 31, no. 11, pp. 1444–1455, Nov. 2008.
- [12] S. Peischl, J. P. Walker, M. Allahmoradi, D. Barrett, R. Gurney, Y. Kerr, E. Kim, J. Le Marshall, C. Rüdiger, D. Ryu, and N. Ye, "Towards validation of SMOS using airborne and ground data over the Murrumbidgee catchment," in *Proc. Int. Congr. MODSIM*, R. S. Anderssen, R. D. Braddock, and L. T. H. Newham, Eds., Jul. 13–17, 2009, pp. 3733–3739.
- [13] O. Merlin, J. P. Walker, A. Chehbouni, and Y. H. Kerr, "Towards deterministic downscaling of SMOS soil moisture using MODIS derived soil evaporative efficiency," *Remote Sens. Environ.*, vol. 112, no. 10, pp. 3935–3946, Oct. 2008.
- [14] R. Panciera, J. P. Walker, J. D. Kalma, E. J. Kim, K. Saleh, and J. P. Wigneron, "Evaluation of the SMOS L-MEB passive microwave soil moisture retrieval algorithm," *Remote Sens. Environ.*, vol. 113, no. 2, pp. 435–444, Feb. 2009.
- [15] K. Saleh, Y. Kerr, P. Richaume, M. Escorihuela, R. Panciera, S. Delwart, G. Boulet, P. Maisongrande, J. P. Walker, P. Wursteisen, and J. P. Wigneron, "Soil moisture retrievals at L-band using a two-step inversion approach (COSMOS/NAFE'05 Experiment)," *Remote Sens. Environ.*, vol. 113, no. 6, pp. 1304–1312, Jun. 2009.
- [16] I. Mladenova, V. Lakshmi, J. P. Walker, R. Panciera, R. W. Wagner, and M. Doubkova, "Validation of the ASAR Global Monitoring mode soil moisture product using the NAFE05 data set," *IEEE Trans. Geosci. Remote Sens.*, vol. 48, no. 6, pp. 2498–2508, Jun. 2010.
- [17] T. J. Jackson, "Multiple resolution analysis of L-band brightness temperature for soil moisture," *IEEE Trans. Geosci. Remote Sens.*, vol. 39, no. 1, pp. 151–164, Jan. 2001.
- [18] Bureau of Rural Sciences (now called Australian Bureau of Agricultural and Resource Economics and Sciences), Landuse Map v3 (last accessed Feb. 3, 2011). [Online]. Available: <http://adl.brs.gov.au/mapserv/landuse/>
- [19] K. H. Northcote, "Atlas of Australian Soils," Melbourne, Australia, CSIRO and Melbourne Univ. Press, 1960. Sheet 3, (last accessed Feb. 3, 2011). [Online]. Available: <http://www.asris.csiro.au/themes/Atlas.html>